



Published in final edited form as:

*Vis Neurosci.* 2017 January ; 34: E007. doi:10.1017/S0952523817000049.

## THALAMOCORTICAL PROCESSING IN VISION

**Reece Mazade and Jose Manuel Alonso**

Department of Biological and Visual Sciences, State University of New York, College of Optometry, New York, New York 10036

### Abstract

Visual information reaches the cerebral cortex through a major thalamocortical pathway that connects the Lateral Geniculate Nucleus (LGN) of the thalamus with the primary visual area of the cortex (area V1). In humans, ~3.4 million afferents from the LGN are distributed within a V1 surface of ~2,400 mm<sup>2</sup>, an afferent number that is reduced by half in the macaque and by more than two orders of magnitude in the mouse. Thalamocortical afferents are sorted in visual cortex based on the spatial position of their receptive fields to form a map of visual space. The visual resolution within this map is strongly correlated with total number of thalamic afferents that V1 receives and the area available to sort them. The ~20,000 afferents of the mouse are only sorted by spatial position because they have to cover a large visual field (~300 degrees) within just 4 mm<sup>2</sup> of V1 area. By contrast, the ~500,000 afferents of the cat are also sorted by eye input and light/dark polarity because they cover a smaller visual field (~200 degrees) within a much larger V1 area (~400 mm<sup>2</sup>), a sorting principle that is likely to apply also to macaques and humans. The increased precision of thalamic sorting allows building multiple copies of the V1 visual map for left/right eyes and light/dark polarities, which become interlaced to keep neurons representing the same visual point close together. In turn, this interlaced arrangement makes cortical neurons with different preferences for stimulus orientation to rotate around single cortical points forming a pinwheel pattern that allows more efficient processing of objects and visual textures.

### Keywords

thalamus; cortex; primary visual cortex; lateral geniculate nucleus

---

The ability to resolve image detail is an important visual function that animals use to guide their behaviors and survive in their environments. Visual acuity can be maximized by increasing the size of the eye to enlarge the images that are projected on the photoreceptor array. The eye size of vertebrates increases with body size and its axial length can range from just 1 mm in the American toad to 107 mm in the blue whale (Hughes 1977; Howland, Merola et al. 2004). Eye size also increases with other factors such as maximum running speed probably to fulfill an important visual function, which is to avoid collisions when moving (Hughes 1977; Heard-Booth and Kirk 2012). When comparing animals with similar size, the fast cheetah (110 Km/h) has the eyes with the largest axial length among carnivores (37 mm) while the flightless penguins have the smallest among birds (21 mm). In primates,

the fastest monkey (patas monkey, 55 Km/h) has eyes with axial lengths (22.5 mm) that are comparable to much bigger primates such as gorillas (22.5 mm) and humans (25 mm) (Howland, Merola et al. 2004; Heard-Booth and Kirk 2012).

## Cortical visual acuity

Among animals with similar eye size, visual acuity increases as a function of photoreceptor density and the number of axons from retinal ganglion cells leaving the optic nerve. Moreover, as the diameter of the optic nerve increases, the volume of the visual thalamus and primary visual cortex also becomes larger. Data from seven different mammals indicate that the primary visual cortex increases by roughly 800 mm<sup>2</sup> for every million of LGN neurons (Figure 1, top left). The relation is ~400 mm<sup>2</sup> for ~0.5 million in cats, ~1,200 mm<sup>2</sup> for ~1.5 million in macaques, and ~2,400 mm<sup>2</sup> for ~3 million in humans (Table 1). Cortical visual acuity for central vision also increases with the number of LGN neurons (Figure 1 top right, ~2 cpd for one million), the size of the V1 area (Figure 1 bottom left, ~2 cpd for 1,000 mm<sup>2</sup>) and the horizontal extent of the binocular visual field (Figure 1 bottom right, ~2 cpd for 50%). The relation between cortical visual acuity and binocular vision is consistent with ecological studies demonstrating a tendency for active predators with frontal eyes to have higher visual acuity than herbivores with lateral eyes (Veilleux and Kirk 2014).

As the number of LGN neurons increases, the number of V1 neurons also increases but the relation is not linear (Stevens 2001). V1 becomes larger than what would be expected from an equal expansion of thalamus and visual cortex. This overexpansion of area V1 makes the density of LGN axons per mm<sup>2</sup> of cortical area to be lower in animals with larger V1 areas. The density is ~4 times lower for the ~1.3 million afferents of macaques (1,093 axons per mm<sup>2</sup>) and the ~3.4 million afferents of humans (1,417 axons per mm<sup>2</sup>) than the ~20,000 LGN afferents of the mouse (5,000 axons per mm<sup>2</sup>) as shown in Table 1. The close relation between V1 size and LGN afferent number could explain why cortical visual acuity is better related with the number of LGN afferents ( $R^2=0.98$ , Figure 1) than the retinal area ( $R^2=0.70$ ), number of retinal ganglion cells ( $R^2=0.54$ ), or even the peak density of retinal ganglion cells ( $R^2=0.67$ ), as can be verified by comparing the values from Tables 1 and 2. For example, cortical visual acuity is ~4 times higher in cats than rabbits (Table 2) but their retinal areas are similar (498 mm<sup>2</sup> in rabbits versus 500 mm<sup>2</sup> in cats, Table 1) and the number of retinal ganglion cells is actually ~2 times higher in rabbits (Table 1). Such discrepancies between retinal resources and visual cortical acuity are likely to be less pronounced among animals of the same species. For example, Spanish wildcats, *Felis silvestris tartessia*, have higher central cone densities, higher peak density of retinal ganglion cells, more axons in the optic nerve, and more LGN neurons than domestic cats of similar weights (Williams, Cavada et al. 1993) and, since cortical visual acuity is strongly correlated with the number of LGN afferents ( $R^2=0.98$ , Figure 1), Spanish wildcats should also have higher cortical visual acuity than domestic cats. Therefore, while the number of retinal ganglion cells is a good predictor of cortical visual acuity when comparing animals that are closely related, the number of LGN afferents is a better predictor when comparing species with different visual needs such as rabbits and cats. The mismatch between cortical visual acuity and retinal ganglion cell number is likely explained by differences in visual behavior. Although rabbits have more retinal ganglion cells than cats, most of these cells are likely to

serve other functions than visual acuity, such as generating quick reflexes to run away from moving targets that abruptly enter their extensive visual field (Table 2) or avoiding collisions when running at fast speeds away from predators. Cats have fewer retinal ganglion cells than rabbits but more of them project to the LGN (Wassle and Illing 1980; Vaney, Peichl et al. 1981), which explains why the LGN volume is ~3 times larger (Table 1) and the cortical visual acuity ~4 times higher in cats than rabbits (Table 2).

While the extent of the rabbit visual field is enormous and approaches 360 degrees ((Hughes 1971), Table 2), animals that need to hunt for prey (or search for small fruits) compromise the size of their visual fields to enhance binocular vision and visual acuity. This evolutionary process explains the strong correlation between cortical visual acuity and binocular field size (Figure 1) and why the ratio between V1 size and visual field size is two orders of magnitude larger in macaques (5.95 mm<sup>2</sup>/deg) than mice (0.01 mm<sup>2</sup>/deg, Table 2). Because LGN central receptive fields are much larger in mice (6.5 deg., Table 2) than macaques (0.09 deg. in parafovea and even smaller in fovea), tiling a horizontal line across the mouse visual field can be done with just 49 LGN receptive fields but it requires 2,222 LGN parafoveal receptive fields in the macaque (Table 2, Figure 2a). Similarly, a horizontal line across the binocular field requires just 6 LGN receptive fields in the mouse but 1,556 in the macaque (Table 2). Interestingly, cortical visual acuity is slightly better correlated with the number of receptive fields required to tile a horizontal line in the binocular field (Table 2,  $R^2 = 0.87$ , power law with 1.27 exponent) than the tiling for the entire visual field ( $R^2 = 0.74$ , power law with 0.79 exponent), which highlights once more the intimate relation between binocular vision and cortical visual acuity.

## Overexpansion of the V1 thalamocortical network

Although the reduction in LGN receptive field size from mice to macaques is remarkable, the overexpansion of area V1 is even more pronounced. The ratio between V1 size and LGN receptive field size is almost one order of magnitude larger in the macaque (0.54 mm<sup>2</sup>/RF) than in the mouse (0.08 mm<sup>2</sup>/RF, Table 2) and, because the average area of an LGN axon patch is similar (mice: 0.24 mm<sup>2</sup>, macaques: 0.23 mm<sup>2</sup>, averaging all axons in mouse and parvocellular/magnocellular axons in macaques), the axon patches of LGN afferents with overlapping receptive fields must overlap in mouse cortex but can be horizontally segregated in macaque cortex (Table 3). Similarly, nearly all LGN afferents with overlapping receptive fields project to the same cortical point in rabbits (>90%, (Stoelzel, Bereshpolova et al. 2008)) but at least 40% project to different cortical points in cats ((Jin, Weng et al. 2008; Jin, Wang et al. 2011).

Our understanding of the horizontal organization of the thalamocortical axon patches in cortex is still very limited in great part because reconstructions from single LGN axons are scarce. However, available measurements from macaques (Blasdel and Lund 1983), cats (Freund, Martin et al. 1985; Humphrey, Sur et al. 1985a; Humphrey, Sur et al. 1985b), tree shrews (Fitzpatrick and Raczkowski 1990; Raczkowski and Fitzpatrick 1990), and mice (Antonini, Fagiolini et al. 1999) allow some rough estimates of axon patch coverage and spacing (Table 3). These data indicate that just 17 non-overlapping LGN-axon-patches are enough to tile a line across area V1 in mice but 5,170 are needed to tile a line across area V1

in macaques (Table 3, Figure 2b). Consequently, the largest horizontal separation between two LGN axon patches with overlapping receptive fields is less than one axon patch in mice but ~2 axon patches in tree shrews, cats, and macaques (Table 3, Figure 2c).

Based on these estimates, we propose that frequent separating gaps between axon patches of LGN afferents with overlapping receptive fields are a unique feature of animals with high visual acuity and have important consequences for the organization of visual cortical maps. In mice, area V1 is not large enough to allow many horizontal gaps between thalamic axon patches with overlapping receptive fields (Table 3) and the density of thalamic afferents is very high (5,000 axons/mm<sup>2</sup>, Table 1). In contrast, area V1 in macaques and cats can accommodate many thalamic afferents with overlapping receptive fields that do not have overlapped patches in cortex (Table 3) and the density of thalamic afferents is ~5 times lower than in mice (Table 1). The separating gaps between LGN axon patches with overlapping receptive fields allow sorting the thalamic afferents within the cortex by functional properties that are not just spatial position but also eye input and dark/light polarity. We argue that this more precise thalamic sorting causes a major reorganization of the visual cortical map.

### Pinwheel cortical maps for stimulus orientation

The spacing between thalamic axon patches with overlapping receptive fields is large enough in primates, carnivores, and scandentia (~2 axon patches, Table 3) to allow clustering afferents of the same type within different cortical domains (e.g. by eye input and contrast polarity). As demonstrated by recent results (Kremkow, Jin et al. 2016; Lee, Huang et al. 2016), these thalamic clusters tend to rotate around each other probably to minimize the amount of wiring and cortical volume needed to represent each visual point (Mitchison 1991; Cajal 1995; Chklovskii, Schikorski et al. 2002). For example, changes in orientation preference within a horizontal track of cat visual cortex are associated with modest changes in receptive field position for one contrast polarity (OFF in Figure 3, top row of receptive fields) and a rotation in receptive field position for the opposite polarity (ON in Figure 3, middle row of receptive fields). In this example, the OFF receptive fields anchor the spatial position represented at the cortical domain while the ON receptive fields rotate with the changes in orientation preference (Figure 3, bottom row of receptive fields).

It remains unknown if such ON-OFF rotation in receptive field position is due to the mosaic organization of ON and OFF ganglion cells in the retina (Wassle, Boycott et al. 1981; Soodak 1987; Paik and Ringach 2011) or the stronger correlated firing between ON and OFF thalamic afferents (Goodhill 1993; Miller 1994; Goodhill and Lowel 1995; Nakagama, Saito et al. 2000). However, it is now clear that the ON-OFF receptive field rotation is closely related (Kremkow, Jin et al. 2016; Lee, Huang et al. 2016) to the pinwheel organization of cortical orientation maps (Figure 4, (Bonhoeffer and Grinvald 1991; Blasdel 1992; Bosking, Zhang et al. 1997; Ohki, Chung et al. 2006)), and that such pinwheel organization allows a more efficient processing of visual textures in animals with high visual acuity (Goris, Simoncelli et al. 2015; Koch, Jin et al. 2016). Therefore, given different orientations represented on the cortical surface the close relationship between visual acuity, ON-OFF receptive field position and the pinwheel organization of cortical

orientation preference, we would like to propose that pinwheel orientation maps originate when area V1 expands enough to generate high visual acuity and thalamic clustering by eye input and ON-OFF polarity.

While this proposal still needs to be rigorously tested, it is consistent with available data. First, as shown here, pinwheel orientation maps emerge as cortical visual acuity increases and area V1 becomes larger (Table 2, Figure 2d). Second, pinwheel orientation maps are not restricted to mammals but include other animals with high visual acuity. For example, barn owls have similar visual acuity to cats (Orlowski, Harmening et al. 2012) and also have pinwheel orientation maps in their visual Wulst, the avian brain structure that receives the bulk of thalamic afferents (Liu and Pettigrew 2003). Third, all animals that have thalamic afferents sorted by eye input in area V1 (ocular dominance columns) also have pinwheel orientation maps, and the spacing between ocular dominance and pinwheel centers is remarkably similar (Table 4). Interestingly, the spacing of both ocular dominance columns and pinwheel centers is narrowly restricted to a range of about 0.4 to 0.5 mm in most animals (Table 4), and the thalamic clusters representing a single whisker in the somatosensory cortex of rodents and lagomorphs are also ~0.5 mm wide (Woolsey and Van der Loos 1970; Bosman, Houweling et al. 2011), which suggests a common organizing principle of sensory cortical topography. Moreover, although the thalamic axon spacing is narrowly constrained to 0.4-0.5 millimeters in most animals, exceptions of larger spacing (wider ocular dominance columns) are usually associated with larger distance between pinwheel centers (Table 4). For example, the cat visual cortex has several areas receiving thalamic input, and the area that has the wider ocular dominance columns, area 18, has also the larger pinwheel spacing (Table 4). Our proposal also predicts that the direction maps in the superior colliculus of frogs implanted with a third eye should be organized in a pinwheel pattern because ocular dominance bands emerge with the arrival of inputs from the third eye (Constantine-Paton and Law 1978), however, this prediction has not yet been tested.

Pinwheel orientation maps are found in animals with large V1 areas and LGN volumes such as macaques (1,189 mm<sup>2</sup>, 77 mm<sup>3</sup>) and cats (380 mm<sup>2</sup>, 19.4 mm<sup>3</sup>) but also in tree shrews, which have a much smaller LGN volume than rabbits (2.4 mm<sup>3</sup> versus 6 mm<sup>3</sup>, Table 1). In spite of their small LGN volume, however, tree shrews are more similar to carnivores and primates than lagomorphs in that they have large binocular fields of vision and low V1 thalamic density. The binocular field of tree shrews is similar to ferrets and two times larger than rabbits (60 degrees, Table 2), and their V1 thalamic density is lower than in ferrets, rabbits and mice (1,515 axons/mm<sup>2</sup>, Table 1). The thalamic axon patches of tree shrews also have a remarkably small area (0.08 mm<sup>2</sup>, Table 3), which is almost as small as the parvocellular axon patches of the macaque (0.07 mm<sup>2</sup>, (Blasdel and Lund 1983)). The thalamocortical organization of the tree shrew is very intriguing and, in many aspects, is radically different from that of primates, carnivores, lagomorphs, and rodents. The thalamic axon patches of tree shrews are extremely asymmetric in shape; they can spread as much 0.9 mm in the lateral dimension but only 0.14 mm in the anteroposterior dimension (Raczkowski and Fitzpatrick 1990). They also show a pronounced inter-ocular asymmetry, with thalamic axons from the ipsilateral eye being 3 times wider in lateral extent (and less abundant) than axons from the contralateral eye (Raczkowski and Fitzpatrick 1990). Finally, the thalamic afferents of tree shrews are segregated by eye input and ON-OFF polarity

through the depth of the middle layers of the cortex instead of horizontally as in carnivores and primates (Harting, Diamond et al. 1973; Hubel 1975; Norton, Rager et al. 1985).

It is unclear why the thalamocortical pathway of tree shrews is so different. An attractive hypothesis is that cortical maps are optimized to keep all thalamic axons with overlapping receptive fields as close as possible within area V1 (Hubel and Wiesel 1977; Durbin and Mitchison 1990; Swindale, Shoham et al. 2000; Carreira-Perpinan and Goodhill 2002; Kremkow, Jin et al. 2016), and this optimization requires different compromises in different animals. Perhaps, because area V1 in tree shrews is so small (66 mm<sup>2</sup>, Table 1), the best compromise is to make the thalamic axon patches as restricted as possible, sort them through the depth of layer 4, and reduce the number of ipsilateral axons while compensating the reduction by increasing its patch size. Carnivores may reach a different compromise to have both high visual acuity to search for prey and high-quality vision while running at fast speeds to hunt (110 Km/h in the cheetah). The best compromise for cats may be to accommodate thalamic afferents in separate cortical areas, a large one specialized in visual acuity (area 17: 380 mm<sup>2</sup>, (Tusa, Palmer et al. 1978)) and a smaller one specialized in processing fast movement (area 18: 98 mm<sup>2</sup>, (Tusa, Rosenquist et al. 1979)). Because running creates motion blur, cats may have a special need for Y thalamic afferents with large receptive fields and fast response latencies (Cleland, Dubin et al. 1971) that are also common in other animals including rodents, lagomorphs, scandentia (Sherman, Norton et al. 1975; Swadlow and Weyand 1985; Price and Morgan 1987; Krahe, El-Danaf et al. 2011), and primates (Schiller and Malpeli 1978; Kaplan and Shapley 1982). However, the receptive fields of Y afferents projecting to area 18 in cats are 2-3 times larger than those from afferents projecting to area 17 (Yeh, Stoelzel et al. 2003). Therefore, such Y afferents would have to cover a huge cortical region if they projected to area 17 (~2 mm<sup>2</sup>/deg, Table 2) but can remain more restricted (although still large) within area 18, which is ~4 times smaller and has a much coarser retinotopic precision (~0.5 mm<sup>2</sup>/deg). Interestingly, in spite of such unique cortical specialization, thalamic axon patches are larger in cats than in any other animal studied to date (Table 3, Figure 2).

## Concluding remarks

The thalamocortical pathway plays an important role in building visual cortical maps and maximizing visual spatial resolution within the cerebral cortex. During evolution, the expansion of primary visual cortex is associated with an increase in visual acuity, a reduction in the cortical density of thalamic afferents, and an increase in the cortical separation between axon patches of thalamic afferents with overlapping receptive fields. This increased separation allows sorting thalamic afferents within the visual cortex not only by their spatial position but also by their eye input and contrast polarity (ON or OFF). We propose that this increased separation between thalamic axon patches, and the resulting thalamic sorting, leads to a major reorganization of the visual cortical map and allows for the emergence of a pinwheel pattern in the cortical representation of stimulus orientation. While this proposal is consistent with available data, anatomical reconstructions from single thalamic axons remain unfortunately scarce, which limits our ability to build realistic models of cortical architecture. It is surprising that, in the era of the connectome, we still have to rely on heroic reconstructions from single thalamic axons obtained more than two decades

ago with more limited resources. Advancing progress in understanding thalamocortical processing would greatly benefit from a renewed effort to fully reconstruct the thalamocortical network, which provides the structural framework for visual function.

## Acknowledgments

Supported by NIH grants EY027157 (RM) and EY05253 (JMA)

## References

- Adams DL, Horton JC. Capricious expression of cortical columns in the primate brain. *Nature neuroscience*. 2003; 6(2):113–114. [PubMed: 12536211]
- Adams DL, Sincich LC, et al. Complete pattern of ocular dominance columns in human primary visual cortex. *The Journal of neuroscience : the official journal of the Society for Neuroscience*. 2007; 27(39):10391–10403. [PubMed: 17898211]
- Andrews TJ, Halpern SD, et al. Correlated size variations in human visual cortex, lateral geniculate nucleus, and optic tract. *The Journal of neuroscience : the official journal of the Society for Neuroscience*. 1997; 17(8):2859–2868. [PubMed: 9092607]
- Antonini A, Fagiolini M, et al. Anatomical correlates of functional plasticity in mouse visual cortex. *The Journal of neuroscience : the official journal of the Society for Neuroscience*. 1999; 19(11):4388–4406. [PubMed: 10341241]
- Baker GE, Thompson ID, et al. Spatial-frequency tuning and geniculocortical projections in the visual cortex (areas 17 and 18) of the pigmented ferret. *The European journal of neuroscience*. 1998; 10(8):2657–2668. [PubMed: 9767395]
- Bezdudnaya T, Cano M, et al. Thalamic burst mode and inattention in the awake LGNd. *Neuron*. 2006; 49(3):421–432. [PubMed: 16446145]
- Blasdel GG. Orientation selectivity, preference, and continuity in monkey striate cortex. *The Journal of neuroscience : the official journal of the Society for Neuroscience*. 1992; 12(8):3139–3161. [PubMed: 1322982]
- Blasdel GG, Lund JS. Termination of afferent axons in macaque striate cortex. *The Journal of neuroscience : the official journal of the Society for Neuroscience*. 1983; 3(7):1389–1413. [PubMed: 6864254]
- Bonhoeffer T, Grinvald A. Iso-orientation domains in cat visual cortex are arranged in pinwheel-like patterns. *Nature*. 1991; 353(6343):429–431. [PubMed: 1896085]
- Bonhoeffer T, Grinvald A. The layout of iso-orientation domains in area 18 of cat visual cortex: optical imaging reveals a pinwheel-like organization. *The Journal of neuroscience : the official journal of the Society for Neuroscience*. 1993; 13(10):4157–4180. [PubMed: 8410182]
- Bonhoeffer T, Kim DS, et al. Optical imaging of the layout of functional domains in area 17 and across the area 17/18 border in cat visual cortex. *The European journal of neuroscience*. 1995; 7(9):1973–1988. [PubMed: 8528473]
- Bosking WH, Zhang Y, et al. Orientation selectivity and the arrangement of horizontal connections in tree shrew striate cortex. *The Journal of neuroscience : the official journal of the Society for Neuroscience*. 1997; 17(6):2112–2127. [PubMed: 9045738]
- Bosman LW, Houweling AR, et al. Anatomical pathways involved in generating and sensing rhythmic whisker movements. *Frontiers in integrative neuroscience*. 2011; 5:53. [PubMed: 22065951]
- Cai D, DeAngelis GC, et al. Spatiotemporal receptive field organization in the lateral geniculate nucleus of cats and kittens. *Journal of neurophysiology*. 1997; 78(2):1045–1061. [PubMed: 9307134]
- Cajal, SR. *Histology of the Nervous System*. Vol. 1. New York: Oxford University Press; 1995.
- Carreira-Perpinan MA, Goodhill GJ. Are visual cortex maps optimized for coverage? *Neural computation*. 2002; 14(7):1545–1560. [PubMed: 12079545]
- Chklovskii DB, Schikorski T, et al. Wiring optimization in cortical circuits. *Neuron*. 2002; 34(3):341–347. [PubMed: 11988166]

- Cleland BG, Dubin MW, et al. Sustained and transient neurones in the cat's retina and lateral geniculate nucleus. *The Journal of physiology*. 1971; 217(2):473–496. [PubMed: 5097609]
- Connolly M, Van Essen D. The representation of the visual field in parvicellular and magnocellular layers of the lateral geniculate nucleus in the macaque monkey. *The Journal of comparative neurology*. 1984; 226(4):544–564. [PubMed: 6747034]
- Constantine-Paton M, Law MI. Eye-specific termination bands in tecta of three-eyed frogs. *Science*. 1978; 202(4368):639–641. [PubMed: 309179]
- Conway JL, Schiller PH. Laminar organization of tree shrew dorsal lateral geniculate nucleus. *Journal of neurophysiology*. 1983; 50(6):1330–1342. [PubMed: 6663330]
- Curcio CA, Allen KA. Topography of ganglion cells in human retina. *The Journal of comparative neurology*. 1990; 300(1):5–25. [PubMed: 2229487]
- De Valois RL, Albrecht DG, et al. Spatial frequency selectivity of cells in macaque visual cortex. *Vision research*. 1982; 22(5):545–559. [PubMed: 7112954]
- Drager UC. Receptive fields of single cells and topography in mouse visual cortex. *The Journal of comparative neurology*. 1975; 160(3):269–290. [PubMed: 1112925]
- Drager UC, Olsen JF. Ganglion cell distribution in the retina of the mouse. *Investigative ophthalmology & visual science*. 1981; 20(3):285–293. [PubMed: 6162818]
- Drenhaus U, von Gunten A, et al. Classes of axons and their distribution in the optic nerve of the tree shrew (*Tupaia belangeri*). *The Anatomical record*. 1997; 249(1):103–116. [PubMed: 9294655]
- Durbin R, Mitchison G. A dimension reduction framework for understanding cortical maps. *Nature*. 1990; 343(6259):644–647. [PubMed: 2304536]
- Engelmann R, Peichl L. Unique distribution of somatostatin-immunoreactive cells in the retina of the tree shrew (*Tupaia belangeri*). *The European journal of neuroscience*. 1996; 8(1):220–228. [PubMed: 8713466]
- Fitzpatrick D, Raczkowski D. Innervation patterns of single physiologically identified geniculocortical axons in the striate cortex of the tree shrew. *Proceedings of the National Academy of Sciences of the United States of America*. 1990; 87(1):449–453. [PubMed: 1688659]
- Forte JD, Hashemi-Nezhad M, et al. Spatial coding and response redundancy in parallel visual pathways of the marmoset *Callithrix jacchus*. *Visual neuroscience*. 2005; 22(4):479–491. [PubMed: 16212705]
- Freund TF, Martin KA, et al. Innervation of cat visual areas 17 and 18 by physiologically identified X- and Y- type thalamic afferents. I. Arborization patterns and quantitative distribution of postsynaptic elements. *The Journal of comparative neurology*. 1985; 242(2):263–274. [PubMed: 4086666]
- Garrett ME, Nauhaus I, et al. Topography and areal organization of mouse visual cortex. *The Journal of neuroscience : the official journal of the Society for Neuroscience*. 2014; 34(37):12587–12600. [PubMed: 25209296]
- Gautschi M, Clarke PG. Neuronal death in the lateral geniculate nucleus of young ferrets following a cortical lesion: time-course, age dependence and involvement of caspases. *Brain research*. 2007; 1167:20–30. [PubMed: 17678880]
- Goodhill GJ. Topography and ocular dominance: a model exploring positive correlations. *Biological cybernetics*. 1993; 69(2):109–118. [PubMed: 8373882]
- Goodhill GJ, Lowel S. Theory meets experiment: correlated neural activity helps determine ocular dominance column periodicity. *Trends in neurosciences*. 1995; 18(10):437–439. [PubMed: 8545906]
- Goris RL, Simoncelli EP, et al. Origin and Function of Tuning Diversity in Macaque Visual Cortex. *Neuron*. 2015; 88(4):819–831. [PubMed: 26549331]
- Harting JK, Diamond IT, et al. Anterograde degeneration study of the cortical projections of the lateral geniculate and pulvinar nuclei in the tree shrew (*Tupaia glis*). *The Journal of comparative neurology*. 1973; 150(4):393–440. [PubMed: 4727888]
- Heard-Booth AN, Kirk EC. The influence of maximum running speed on eye size: a test of Leuckart's Law in mammals. *Anatomical record*. 2012; 295(6):1053–1062.



- Heesy CP. On the relationship between orbit orientation and binocular visual field overlap in mammals. *The anatomical record Part A, Discoveries in molecular, cellular, and evolutionary biology*. 2004; 281(1):1104–1110.
- Heimel JA, Van Hooser SD, et al. Laminar organization of response properties in primary visual cortex of the gray squirrel (*Sciurus carolinensis*). *Journal of neurophysiology*. 2005; 94(5):3538–3554. [PubMed: 16000528]
- Henderson Z. Distribution of ganglion cells in the retina of adult pigmented ferret. *Brain research*. 1985; 358(1-2):221–228. [PubMed: 4075115]
- Holdefer RN, Norton TT. Laminar organization of receptive field properties in the dorsal lateral geniculate nucleus of the tree shrew (*Tupaia glis*). *The Journal of comparative neurology*. 1995; 358(3):401–413. [PubMed: 7560294]
- Howland HC, Merola S, et al. The allometry and scaling of the size of vertebrate eyes. *Vision research*. 2004; 44(17):2043–2065. [PubMed: 15149837]
- Hubel DH. An autoradiographic study of the retino-cortical projections in the tree shrew (*Tupaia glis*). *Brain research*. 1975; 96(1):41–50. [PubMed: 809108]
- Hubel DH, Wiesel TN. Receptive fields, binocular interaction and functional architecture in the cat's visual cortex. *The Journal of physiology*. 1962; 160:106–154. [PubMed: 14449617]
- Hubel DH, Wiesel TN. Receptive fields and functional architecture of monkey striate cortex. *The Journal of physiology*. 1968; 195(1):215–243. [PubMed: 4966457]
- Hubel DH, Wiesel TN. Ferrier lecture. Functional architecture of macaque monkey visual cortex. *Proceedings of the Royal Society of London Series B, Biological sciences*. 1977; 198(1130):1–59.
- Hughes A. Topographical relationships between the anatomy and physiology of the rabbit visual system. *Documenta Ophthalmologica*. 1971; 30:33–159. [PubMed: 5000058]
- Hughes A. A quantitative analysis of the cat retinal ganglion cell topography. *The Journal of comparative neurology*. 1975; 163(1):107–128. [PubMed: 1159109]
- Hughes, A. The topography of vision in mammals of contrasting life style: Comparative optics and retinal organisation. In: Crescitelli, F., editor. *Handbook of sensory physiology, VII/5: The visual system in vertebrates*. Berlin: Springer-Verlag; 1977. p. 613-756.
- Hughes A, Wassle H. The cat optic nerve: fibre total count and diameter spectrum. *The Journal of comparative neurology*. 1976; 169(2):171–184. [PubMed: 965509]
- Humphrey AL, Norton TT. Topographic organization of the orientation column system in the striate cortex of the tree shrew (*Tupaia glis*). I. Microelectrode recording. *The Journal of comparative neurology*. 1980; 192(3):531–547. [PubMed: 7419743]
- Humphrey AL, Sur M, et al. Projection patterns of individual X- and Y-cell axons from the lateral geniculate nucleus to cortical area 17 in the cat. *The Journal of comparative neurology*. 1985a; 233(2):159–189. [PubMed: 3973100]
- Humphrey AL, Sur M, et al. Termination patterns of individual X- and Y-cell axons in the visual cortex of the cat: projections to area 18, to the 17/18 border region, and to both areas 17 and 18. *The Journal of comparative neurology*. 1985b; 233(2):190–212. [PubMed: 3973101]
- Jeon CJ, Strettoi E, et al. The major cell populations of the mouse retina. *The Journal of neuroscience : the official journal of the Society for Neuroscience*. 1998; 18(21):8936–8946. [PubMed: 9786999]
- Jin J, Wang Y, et al. Population receptive fields of ON and OFF thalamic inputs to an orientation column in visual cortex. *Nature neuroscience*. 2011; 14(2):232–238. [PubMed: 21217765]
- Jin JZ, Weng C, et al. On and off domains of geniculate afferents in cat primary visual cortex. *Nature neuroscience*. 2008; 11(1):88–94. [PubMed: 18084287]
- Johnson EN, Van Hooser SD, et al. The representation of S-cone signals in primary visual cortex. *The Journal of neuroscience : the official journal of the Society for Neuroscience*. 2010; 30(31):10337–10350. [PubMed: 20685977]
- Kaas JH, Hall WC, et al. Visual cortex of the tree shrew (*Tupaia glis*): architectonic subdivisions and representations of the visual field. *Brain research*. 1972; 42(2):491–496. [PubMed: 5050179]
- Kaplan E, Shapley RM. X and Y cells in the lateral geniculate nucleus of macaque monkeys. *The Journal of physiology*. 1982; 330:125–143. [PubMed: 7175738]

- Kim CB, Tom BW, et al. Effects of aging on the densities, numbers, and sizes of retinal ganglion cells in rhesus monkey. *Neurobiology of aging*. 1996; 17(3):431–438. [PubMed: 8725905]
- Koch E, Jin J, et al. Functional implications of orientation maps in primary visual cortex. *Nature communications*. 2016; 7:13529.
- Kong X, Wang K, et al. Comparative study of the retinal vessel anatomy of rhesus monkeys and humans. *Clinical & experimental ophthalmology*. 2010; 38(6):629–634. [PubMed: 20584020]
- Krahe TE, El-Danaf RN, et al. Morphologically distinct classes of relay cells exhibit regional preferences in the dorsal lateral geniculate nucleus of the mouse. *The Journal of neuroscience : the official journal of the Society for Neuroscience*. 2011; 31(48):17437–17448. [PubMed: 22131405]
- Kremkow J, Jin J, et al. Principles underlying sensory map topography in primary visual cortex. *Nature*. 2016; 533(7601):52–57. [PubMed: 27120164]
- Law MI, Zaksas KR, et al. Organization of primary visual cortex (area 17) in the ferret. *The Journal of comparative neurology*. 1988; 278(2):157–180. [PubMed: 3068264]
- Lee KS, Huang X, et al. Topology of ON and OFF inputs in visual cortex enables an invariant columnar architecture. *Nature*. 2016; 533(7601):90–94. [PubMed: 27120162]
- Levitt JB, Schumner RA, et al. Visual response properties of neurons in the LGN of normally reared and visually deprived macaque monkeys. *Journal of neurophysiology*. 2001; 85(5):2111–2129. [PubMed: 11353027]
- Liu GB, Pettigrew JD. Orientation mosaic in barn owl's visual Wulst revealed by optical imaging: comparison with cat and monkey striate and extra-striate areas. *Brain research*. 2003; 961(1):153–158. [PubMed: 12535788]
- Lowel S. Ocular dominance column development: strabismus changes the spacing of adjacent columns in cat visual cortex. *The Journal of neuroscience : the official journal of the Society for Neuroscience*. 1994; 14(12):7451–7468. [PubMed: 7996187]
- Malpeli JG, Baker FH. The representation of the visual field in the lateral geniculate nucleus of *Macaca mulatta*. *The Journal of comparative neurology*. 1975; 161(4):569–594. [PubMed: 1133232]
- Miller KD. A model for the development of simple cell receptive fields and the ordered arrangement of orientation columns through activity-dependent competition between ON- and OFF-center inputs. *The Journal of neuroscience : the official journal of the Society for Neuroscience*. 1994; 14(1):409–441. [PubMed: 8283248]
- Mitchison G. Neuronal branching patterns and the economy of cortical wiring. *Proceedings Biological sciences*. 1991; 245(1313):151–158. [PubMed: 1682939]
- Movshon JA, Thompson ID, et al. Spatial and temporal contrast sensitivity of neurones in areas 17 and 18 of the cat's visual cortex. *The Journal of physiology*. 1978; 283:101–120. [PubMed: 722570]
- Muly EC, Fitzpatrick D. The morphological basis for binocular and ON/OFF convergence in tree shrew striate cortex. *The Journal of neuroscience : the official journal of the Society for Neuroscience*. 1992; 12(4):1319–1334. [PubMed: 1313492]
- Murphy EH, Berman N. The rabbit and the cat: a comparison of some features of response properties of single cells in the primary visual cortex. *The Journal of comparative neurology*. 1979; 188(3):401–427. [PubMed: 489801]
- Najdzion J, Wasilewska B, et al. A morphometric comparative study of the lateral geniculate body in selected placental mammals: the common shrew, the bank vole, the rabbit, and the fox. *Folia morphologica*. 2009; 68(2):70–78. [PubMed: 19449292]
- Nakagama H, Saito T, et al. Effect of imbalance in activities between ON- and OFF-center LGN cells on orientation map formation. *Biological cybernetics*. 2000; 83(2):85–92. [PubMed: 10966048]
- Niell CM, Stryker MP. Highly selective receptive fields in mouse visual cortex. *The Journal of neuroscience : the official journal of the Society for Neuroscience*. 2008; 28(30):7520–7536. [PubMed: 18650330]
- Norton TT, Rager G, et al. ON and OFF regions in layer IV of striate cortex. *Brain research*. 1985; 327(1-2):319–323. [PubMed: 2985176]
- Obermayer K, Blasdel GG. Geometry of orientation and ocular dominance columns in monkey striate cortex. *The Journal of neuroscience : the official journal of the Society for Neuroscience*. 1993; 13(10):4114–4129. [PubMed: 8410181]

- Obermayer K, Blasdel GG. Singularities in primate orientation maps. *Neural computation*. 1997; 9(3): 555–575. [PubMed: 9097474]
- Ohki K, Chung S, et al. Highly ordered arrangement of single neurons in orientation pinwheels. *Nature*. 2006; 442(7105):925–928. [PubMed: 16906137]
- Orlowski J, Harmening W, et al. Night vision in barn owls: visual acuity and contrast sensitivity under dark adaptation. *Journal of vision*. 2012; 12(13):4.
- Oyster CW, Takahashi ES, et al. Density, soma size, and regional distribution of rabbit retinal ganglion cells. *The Journal of neuroscience : the official journal of the Society for Neuroscience*. 1981; 1(12):1331–1346. [PubMed: 7320749]
- Paik SB, Ringach DL. Retinal origin of orientation maps in visual cortex. *Nature neuroscience*. 2011; 14(7):919–925. [PubMed: 21623365]
- Perry VH, Cowey A. The ganglion cell and cone distributions in the monkey's retina: implications for central magnification factors. *Vision research*. 1985; 25(12):1795–1810. [PubMed: 3832605]
- Petry HM, Fox R, et al. Spatial contrast sensitivity of the tree shrew. *Vision research*. 1984; 24(9): 1037–1042. [PubMed: 6506467]
- Price DJ, Morgan JE. Spatial properties of neurones in the lateral geniculate nucleus of the pigmented ferret. *Experimental brain research*. 1987; 68(1):28–36. [PubMed: 3691695]
- Raczkowski D, Fitzpatrick D. Terminal arbors of individual, physiologically identified geniculocortical axons in the tree shrew's striate cortex. *The Journal of comparative neurology*. 1990; 302(3):500–514. [PubMed: 1702114]
- Rao SC, Toth LJ, et al. Optically imaged maps of orientation preference in primary visual cortex of cats and ferrets. *The Journal of comparative neurology*. 1997; 387(3):358–370. [PubMed: 9335420]
- Roe AW, Fritsches K, et al. Optical imaging of functional organization of V1 and V2 in marmoset visual cortex. *The anatomical record Part A, Discoveries in molecular, cellular, and evolutionary biology*. 2005; 287(2):1213–1225.
- Schiller PH, Malpel JG. Functional specificity of lateral geniculate nucleus laminae of the rhesus monkey. *Journal of neurophysiology*. 1978; 41(3):788–797. [PubMed: 96227]
- Scholl B, Burge J, et al. Binocular integration and disparity selectivity in mouse primary visual cortex. *Journal of neurophysiology*. 2013; 109(12):3013–3024. [PubMed: 23515794]
- Seecharan DJ, Kulkarni AL, et al. Genetic control of interconnected neuronal populations in the mouse primary visual system. *The Journal of neuroscience : the official journal of the Society for Neuroscience*. 2003; 23(35):11178–11188. [PubMed: 14657177]
- Selemon LD, Begovic A. Stereologic analysis of the lateral geniculate nucleus of the thalamus in normal and schizophrenic subjects. *Psychiatry research*. 2007; 151(1-2):1–10. [PubMed: 17383740]
- Sesma MA, Casagrande VA, et al. Cortical connections of area 17 in tree shrews. *The Journal of comparative neurology*. 1984; 230(3):337–351. [PubMed: 6520238]
- Sherman SM. Permanence of visual perimetry deficits in monocularly and binocularly deprived cats. *Brain research*. 1974; 73(3):491–501. [PubMed: 4835370]
- Sherman SM, Norton TT, et al. X- and Y-cells in the dorsal lateral geniculate nucleus of the tree shrew (*Tupaia glis*). *Brain research*. 1975; 93(1):152–157. [PubMed: 806329]
- Soodak RE. The retinal ganglion cell mosaic defines orientation columns in striate cortex. *Proceedings of the National Academy of Sciences of the United States of America*. 1987; 84(11):3936–3940. [PubMed: 3108884]
- Stevens CF. An evolutionary scaling law for the primate visual system and its basis in cortical function. *Nature*. 2001; 411(6834):193–195. [PubMed: 11346795]
- Stoelzel CR, Bereshpolova Y, et al. The impact of an LGNd impulse on the awake visual cortex: synaptic dynamics and the sustained/transient distinction. *The Journal of neuroscience : the official journal of the Society for Neuroscience*. 2008; 28(19):5018–5028. [PubMed: 18463255]
- Swadlow HA, Weyand TG. Receptive-field and axonal properties of neurons in the dorsal lateral geniculate nucleus of awake unparalyzed rabbits. *Journal of neurophysiology*. 1985; 54(1):168–183. [PubMed: 2993538]

- Swindale NV, Shoham D, et al. Visual cortex maps are optimized for uniform coverage. *Nature neuroscience*. 2000; 3(8):822–826. [PubMed: 10903576]
- Takahata T, Miyashita M, et al. Identification of ocular dominance domains in New World owl monkeys by immediate-early gene expression. *Proceedings of the National Academy of Sciences of the United States of America*. 2014; 111(11):4297–4302. [PubMed: 24591618]
- Tang J, Ardila Jimenez SC, et al. Visual Receptive Field Properties of Neurons in the Mouse Lateral Geniculate Nucleus. *PloS one*. 2016; 11(1):e0146017. [PubMed: 26741374]
- Tusa RJ, Palmer LA, et al. The retinotopic organization of area 17 (striate cortex) in the cat. *The Journal of comparative neurology*. 1978; 177(2):213–235. [PubMed: 413845]
- Tusa RJ, Rosenquist AC, et al. Retinotopic organization of areas 18 and 19 in the cat. *The Journal of comparative neurology*. 1979; 185(4):657–678. [PubMed: 447876]
- Vaney DI, Peichl L, et al. Almost all ganglion cells in the rabbit retina project to the superior colliculus. *Brain research*. 1981; 212(2):447–453. [PubMed: 7225878]
- Veilleux CC, Kirk EC. Visual acuity in mammals: effects of eye size and ecology. *Brain, behavior and evolution*. 2014; 83(1):43–53.
- Vitek DJ, Schall JD, et al. Morphology, central projections, and dendritic field orientation of retinal ganglion cells in the ferret. *The Journal of comparative neurology*. 1985; 241(1):1–11. [PubMed: 4056111]
- Wassle H, Boycott BB, et al. Morphology and mosaic of on- and off-beta cells in the cat retina and some functional considerations. *Proceedings of the Royal Society of London Series B, Biological sciences*. 1981; 212(1187):177–195.
- Wassle H, Illing RB. The retinal projection to the superior colliculus in the cat: a quantitative study with HRP. *The Journal of comparative neurology*. 1980; 190(2):333–356. [PubMed: 7381061]
- Williams RW, Cavada C, et al. Rapid evolution of the visual system: a cellular assay of the retina and dorsal lateral geniculate nucleus of the Spanish wildcat and the domestic cat. *The Journal of neuroscience : the official journal of the Society for Neuroscience*. 1993; 13(1):208–228. [PubMed: 8423469]
- Williams RW, Strom RC, et al. Genetic and environmental control of variation in retinal ganglion cell number in mice. *The Journal of neuroscience : the official journal of the Society for Neuroscience*. 1996; 16(22):7193–7205. [PubMed: 8929428]
- Woolsey TA, Van der Loos H. The structural organization of layer IV in the somatosensory region (SI) of mouse cerebral cortex. The description of a cortical field composed of discrete cytoarchitectonic units. *Brain research*. 1970; 17(2):205–242. [PubMed: 4904874]
- Xu X, Bosking W, et al. Functional organization of visual cortex in the owl monkey. *The Journal of neuroscience : the official journal of the Society for Neuroscience*. 2004; 24(28):6237–6247. [PubMed: 15254078]
- Xu X, Bosking WH, et al. Functional organization of visual cortex in the prosimian bush baby revealed by optical imaging of intrinsic signals. *Journal of neurophysiology*. 2005; 94(4):2748–2762. [PubMed: 16000523]
- Yacoub E, Harel N, et al. High-field fMRI unveils orientation columns in humans. *Proceedings of the National Academy of Sciences of the United States of America*. 2008; 105(30):10607–10612. [PubMed: 18641121]
- Yeh CI, Stoelzel CR, et al. Two different types of Y cells in the cat lateral geniculate nucleus. *Journal of neurophysiology*. 2003; 90(3):1852–1864. [PubMed: 12966179]
- Zahs KR, Stryker MP. The projection of the visual field onto the lateral geniculate nucleus of the ferret. *The Journal of comparative neurology*. 1985; 241(2):210–224. [PubMed: 4067015]
- Zhuang J, Stoelzel CR, et al. Layer 4 in primary visual cortex of the awake rabbit: contrasting properties of simple cells and putative feedforward inhibitory interneurons. *The Journal of neuroscience : the official journal of the Society for Neuroscience*. 2013; 33(28):11372–11389. [PubMed: 23843510]

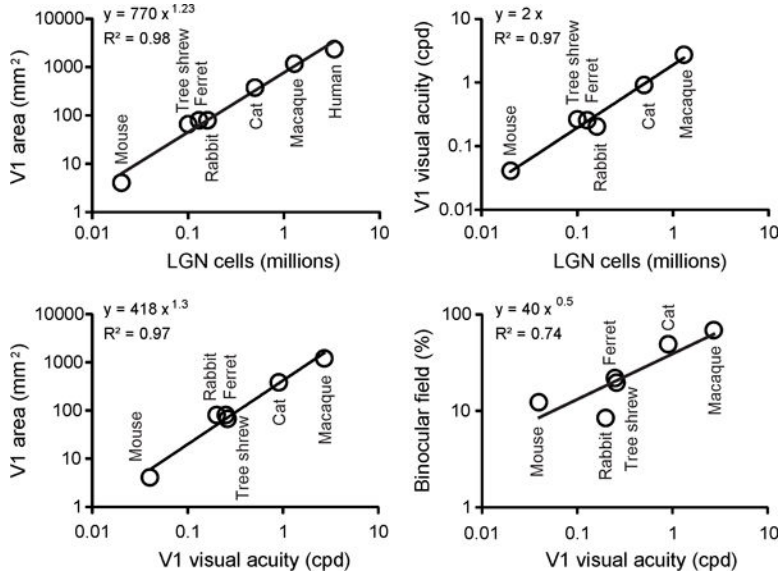


**Figure 1.** Thalamocortical visual function in different animals: primates, carnivores, scandentia, lagomorphs, and rodents. Top. The number of LGN cells is correlated to the size of area V1 (left) and cortical visual acuity (right). Bottom. Cortical visual acuity is also correlated to the size of area V1 (left, expected from correlations shown at the top), and the horizontal extent of the binocular field (shown as a percentage of the total horizontal extent of the visual field). Size of area V1 refers to only one hemisphere. See Table 1 for references.

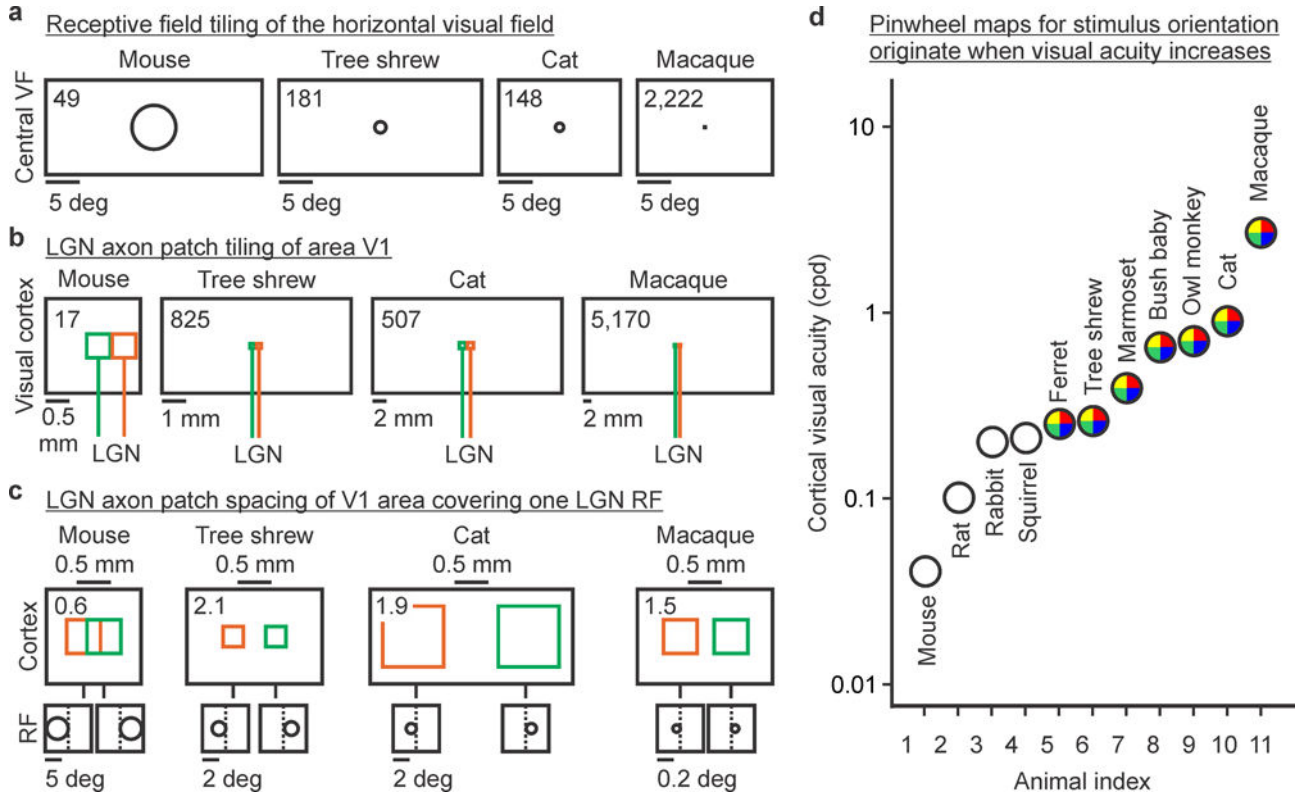


**Figure 2.** Thalamocortical networks underlying the organization of visual cortical maps. **a**, Number of non-overlapping LGN receptive fields needed to tile a horizontal line across the visual field (shown on top left corner of each rectangle, taken from column 7 in Table 2). Only 1/10 of the horizontal visual field is represented for illustration purposes. **b**, Number of non-overlapping LGN-axon-patches needed to tile a horizontal line through area V1 (shown on top left corner of each rectangle, taken from column 3 in Table 3). Green and orange colors represent two different afferents. **c**, The largest spacing between two LGN-axon-patches covering one LGN receptive field in visual cortex (shown on top left corner of each rectangle, taken from column 5 in Table 3). For simplicity, axon patches are represented as squares. **d**, Cortical optimal visual acuity across 11 different species (values obtained from the references cited below). Colored circles indicate pinwheel orientation maps in visual cortex. **Mouse:** (Niell and Stryker 2008). **Rat, Gray squirrel, Bush baby, Owl monkey:** (Heimel, Van Hooser et al. 2005). **Rabbit:** (Zhuang, Stoelzel et al. 2013). **Ferret:** (Baker, Thompson et al. 1998). **Tree shrew:** (Johnson, Van Hooser et al. 2010). **Marmoset:** (Forte, Hashemi-Nezhad et al. 2005). **Cat:** (Movshon, Thompson et al. 1978). **Macaque:** (De Valois, Albrecht et al. 1982). VF: visual field. RF: receptive field

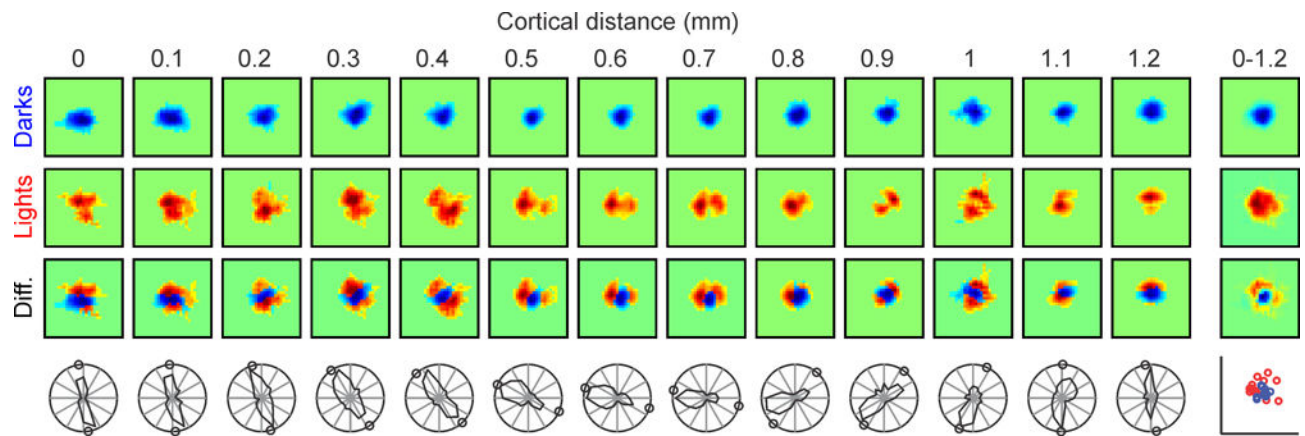


**Figure 3.**

Changes in orientation preference and receptive field position along a horizontal track of cat visual cortex. From top to bottom, the rows show OFF receptive fields mapped with dark stimuli (in blue), ON receptive fields mapped with light stimuli (in red), the ON-OFF receptive field difference (diff.), and the orientation/direction preference measured with moving bars (circles show the orientation preference predicted from the receptive field maps). From left to right, the columns show cortical measurements separated by 0.1 mm from 0 to 1.2 mm distance. The column on the right shows the receptive field average along the entire horizontal track (top three receptive fields) and the central positions of ON (red circles) and OFF receptive fields (blue circles). The position of these ON and OFF cortical receptive fields is determined by the receptive field population of the ON and OFF thalamic afferents.

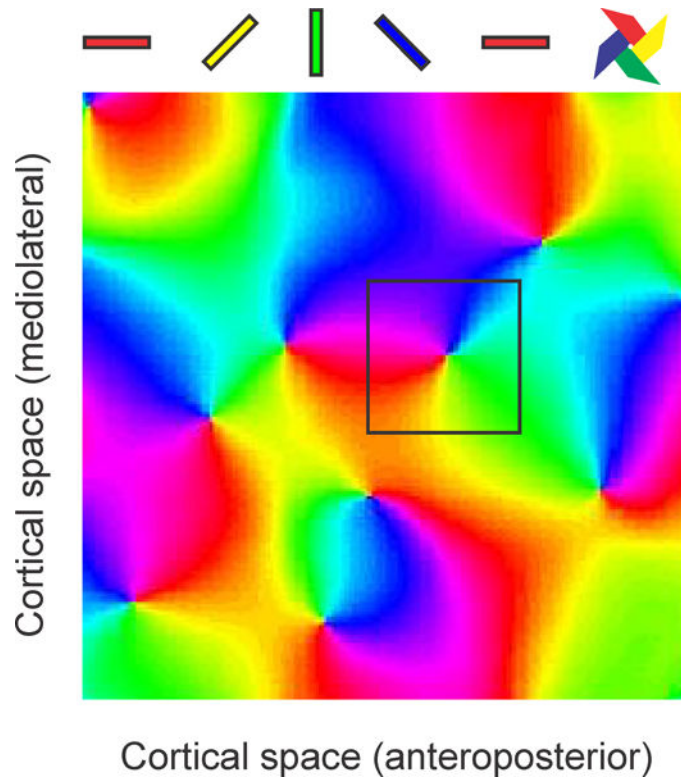


**Figure 4.** Pinwheel pattern of the cortical map for stimulus orientation. Colors illustrate the different orientations represented on the cortical surface (cat area 17,  $2 \times 2$  mm). A square of  $0.5 \times 0.5$  mm is shown centered on a cortical pinwheel.



Comparison of visual systems across different animals: primates, carnivores, scandentia, lagomorphs, and rodents. Columns 1-9 are taken from references cited below. Column 10 is calculated as column 8 times column 9; column 11 is calculated as column 10 divided by column 7; column 12 is calculated as column 6 times one million divided by column 8. Columns are numbered from left to right, from [1] for body weight to [12] for LGN-axon density in V1. **Human:** (Howland, Merola et al. 2004) for [1], [2]; (Curcio and Allen 1990) for [3], [4], [5]; (Selemon and Begovic 2007) for [6]; (Andrews, Halpem et al. 1997) for [7], [8], [10]. **Macaque:** (Howland, Merola et al. 2004) for [1]; (Perry and Cowey 1985) for [2]; (Kong, Wang et al. 2010) for [3]; (Kim, Tom et al. 1996) for [4]; (Perry and Cowey 1985) for [5]; (Connolly and Van Essen 1984) for [6]; (Malpeli and Baker 1975) for [7]; (Adams, Sincich et al. 2007) for [8]; (Hubel and Wiesel 1968) for [9]. **Cat:** (Howland, Merola et al. 2004) for [1], [2]; (Hughes 1975) for [3], [5]; (Hughes and Wassele 1976) for [4]; (Williams, Cavada et al. 1993) for [5], [6], [7]; (Tusa, Palmer et al. 1978) for [8]; (Hubel and Wiesel 1962) for [9]. **Tree shrew:** (Howland, Merola et al. 2004) for [1], [2]; (Hughes 1975) [1], [2]; (Engelmann and Peichl 1996) for [3]; (Drenhaus, von Gunten et al. 1997) for [4]; (Petty, Fox et al. 1984) for [5]; (Conway and Schiller 1983) for [6], [7]; (Sesma, Casagrande et al. 1984) for [8]; (Muly and Fitzpatrick 1992) for [9]. **Ferret:** (Howland, Merola et al. 2004) for [1], [2]; (Henderson 1985) for [3], [4]; (Vitek, Schall et al. 1985) for [5]; (Gautschi and Clarke 2007) for [6]; (Zahs and Stryker 1985) for [7]; (Law, Zahs et al. 1988) for [8], [9]. **Rabbit:** (Howland, Merola et al. 2004) for [1], [2]; (Oyster, Takahashi et al. 1981) for [3], [4], [5]; (Najdzion, Wasilewska et al. 2009) for [6], [7]; (Hughes 1971) for [8], [9]. **Mouse:** (Howland, Merola et al. 2004) for [1], [2]; (Drager and Olsen 1981) for [3]; (Williams, Strom et al. 1996) for [4]; (Jeon, Strettoi et al. 1998) for [5]; (Seecharan, Kulkarni et al. 2003) for [6], [7]; (Garrett, Nauhaus et al. 2014) for [8]; (Antonini, Fagiolini et al. 1999) for [9]. RGC: retinal ganglion cells.

Table 1

Animal	Body weight (kg)	Eye axial length (mm)	Retinal area (mm <sup>2</sup> )	Number of RGC (millions)	Peak RGC density (cells/mm <sup>2</sup> )	Number of LGN cells (millions)	LGN volume (mm <sup>3</sup> )	V1 area (mm <sup>2</sup> )	V1 thickness (mm)	V1 volume (mm <sup>3</sup> )	V1/LGN volume ratio	LGN-axon density in V1 (axons/mm <sup>2</sup> )
Human	72.34	24.52	1,012	1.07	35,100	3.40	118.0	2,399	2.3	5,416	46	1,417
Macaque	9.25	19.60	636	1.54	33,000	1.30	77.0	1,189	2.0	2,378	31	1,093
Cat	3.05	21.94	510	0.19	10,500	0.51	19.4	380	1.8	684	35	1,342
Tree Shrew	0.12	8.07	122	0.57	20,000	0.10	2.4	66	1.4	92	39	1,515
Ferret	0.66	7.50	84	0.08	5,200	0.13	3.7	80	1.8	144	39	1,625
Rabbit	2.72	18.07	498	0.41	5,155	0.16	6.0	80	1.8	144	24	2,000
Mouse	0.03	5.28	15	0.05	3,300	0.02	0.3	4	1.0	4	13	5,000

Table 2

Cortical mapping of visual space in different animals: primates, carnivores, scandentia, lagomorphs, and rodents. Columns 1-2, 5, 9-10 are taken from references cited below. Column 3 is calculated as column 2 divided by column 1 times 100; column 4 is calculated as column 8 from Table 1 divided by column 1 in this table; column 6 is calculated as column 4 times column 5; column 7 is calculated as column 1 divided by column 5; column 8 is calculated as column 2 divided by column 5. Columns are numbered from left to right as in Table 1. ***Macaque***: (Adams, Sincich et al. 2007) for [1], [2]; (Levitt, Schumer et al. 2001) for [5]; (De Valois, Albrecht et al. 1982) for [9]; (Hubel and Wiesel 1968) for [10]. ***Cat***: (Sherman 1974) for [1], [2]; (DeAngelis et al. 1997) for [5]; (Movshon, Thompson et al. 1978) for [9]; (Hubel and Wiesel 1962) for [10]. ***Tree shrew***: (Kaas, Hall et al. 1972) for [1], [2]; (Holdefer and Norton 1995) for [5]; (Johnson, Van Hooser et al. 2010) for [9]; (Humphrey and Norton 1980) for [10]. ***Ferret***: (Law, Zaks et al. 1988) for [1], [2]; (Zaks and Stryker 1985) for [5]; (Baker, Thompson et al. 1998) for [9]; (Law, Zaks et al. 1988) for [10]. ***Rabbit***: (Hughes 1971) for [1], [2]; (Bezudnaya, Cano et al. 2006) for [5]; (Zhuang, Stoelzel et al. 2013) for [9]; (Murphy and Berman 1979) for [10]. ***Mouse***: (Scholl, Burge et al. 2013) for [1]; (Heesy 2004) for [2]; (Tang, Ardila Jimenez et al. 2016) for [5]; (Niell and Stryker 2008) for [9]; (Drager 1975) for [10]. RF: receptive field.

Animal	Horizontal visual field (deg)	Binocular visual field (deg)	Binocular visual field (%)	Cortical area per degree (mm <sup>2</sup> /deg)	Central LGN RF size (deg)	Cortical area per RF (mm <sup>2</sup> /RF)	Number of RFs per horizontal visual field	Number of RFs per binocular visual field	V1 central visual acuity (cpd)	Orientation maps
Macaque	200	140	70	5.95	0.09	0.54	2,222	1,556	2.70	yes
Cat	180	90	50	2.11	1.22	2.58	148	74	0.90	yes
Tree Shrew	300	60	20	0.22	1.66	0.37	181	36	0.26	yes
Ferret	270	60	22	0.30	3.00	0.89	90	20	0.25	yes
Rabbit	350	30	9	0.23	2.20	0.50	159	14	0.20	no
Mouse	320	40	13	0.01	6.50	0.08	49	6	0.04	no

**Table 3**

Comparison of LGN axon-patch density across different animals: primates, carnivores, scandentia, and rodents. Column 1 is taken from references cited below. Column 2 is calculated as the square root of column 1 times 1000; column 3 is calculated as column 8 in Table 1 divided by column 1 in this table; column 4 is calculated as column 6 in Table 1 times column 1 in this table times one million and divided by column 8 in Table 1; column 5 is calculated as the square root of the ratio between column 6 of Table 2 and column 1 of this table. Columns are numbered from left to right as in Table 1. ***Macaque:*** (Blasdel and Lund 1983) for [1]. ***Cat(area 17):*** (a) for [1]. ***Tree shrew:*** (Raczkowski and Fitzpatrick 1990) for [1]. ***Mouse:*** (Antonini, Fagiolini et al. 1999) for [1]. RF: receptive field.

Animal	LGN-axon-patch area (mm <sup>2</sup> )	LGN-axon-patch spread (microns)	Non-overlapping LGN axon-patches per mm <sup>2</sup> of V1	Overlapping LGN axon-patches per V1 point	LGN axon-patch spacing per LGN RF
Macaque	0.23	480	5,170	251	1.5
Cat	0.75	866	507	1,007	1.9
Tree Shrew	0.08	283	825	121	2.1
Mouse	0.24	490	17	1,200	0.6

**Table 4**

Cortical spacing for ocular dominance and orientation pinwheels in primates, carnivores, scandentia and rodents. Column 2 is calculated as the square root of 1/pinwheel density. References for the column on the left [1] and on the right [2] are provided below. **Human:** (Adams, Sincich et al. 2007) for [1]; (Yacoub, Harel et al. 2008) for [2]. **Macaque:** (Adams, Sincich et al. 2007) for [1]; (Obermayer and Blasdel 1993) for [2]. **Cat area 17:** (Lowel 1994) for [1]; (Bonhoeffer, Kim et al. 1995) for [2]. **Cat area 18:** (Lowel 1994) for [1]; (Bonhoeffer and Grinvald 1993) for [2]. **Owl monkey:** (Takahata, Miyashita et al. 2014) for [1]; (Xu, Bosking et al. 2004) for [2]. **Bush baby:** (Xu, Bosking et al. 2005) for [1], [2]. **Marmoset:** (Roe, Fritsches et al. 2005) for [1]; (Liu and Pettigrew 2003) for [2]. **Squirrel monkey:** (Adams and Horton 2003) for [1]; (Obermayer and Blasdel 1997) for [2]. **Ferret:** (Law, Zahs et al. 1988) for [1]; (Rao, Toth et al. 1997) for [2].

Animal	Ocular dominance width (mm)	Pinwheel spacing (mm)
Human	0.84	0.72
Macaque	0.53	0.35
Cat area 17	0.45	0.69
Cat area 18	0.81	0.91
Owl monkey	0.45	0.36
Bush baby	0.53	0.40
Marmoset	0.30	0.46
Squirrel monkey	0.44	0.30
Ferret	0.41	0.43
<b>Average</b>	<b>0.53</b>	<b>0.51</b>
<b>Median</b>	<b>0.45</b>	<b>0.43</b>